Available online at www.sciencedirect.com
SCIENCE DIRECT
Thin Solid Films 497 (2006) 304 – 308
thin solid films
www.elsevier.com/locate/tsf

Growth and characterization of piezoelectric AlN thin films for diamond-based surface acoustic wave devices

M. Benetti [a], D. Cannatà [a], F. Di Pietrantonio [a], E. Verona [a,*], A. Generosi [b], B. Paci [b], V. Rossi Albertini [b]

[a] *C.N.R. Istituto di Acustica "O. M. Corbino", Via del Fosso del Cavaliere 100, 00133 Roma, Italy*
[b] *C.N.R. Istituto di Struttura della Materia, Via del Fosso del Cavaliere 100, 00133 Roma, Italy*

Received 4 April 2005; received in revised form 28 September 2005; accepted 27 October 2005
Available online 6 December 2005

Abstract

We report on the preparation and structural characterization of piezoelectric films of aluminium nitride onto diamond substrates. The samples were fabricated by sequential radio frequency reactive diode sputtering processes, carried out at various temperatures, in a head vacuum system starting from stechiometric targets. The structural characterization of the films was performed by energy dispersive X-ray diffraction analysis. The deposition temperature was found to play a relevant role to obtain highly textured films with the *c*-axis perpendicular to the substrate surface, as required by surface-acoustic-wave applications. In particular, a minimum substrate temperature of 300 °C was needed in order to obtain any internal order along the *c*-axis while, increasing the temperature, the AlN <002> orientation becomes preferential. The rocking curve analysis revealed a good crystalline quality of the AlN films whose degree of epitaxy can be well described by a linearly increasing function of the temperature at which the films are grown.
© 2005 Elsevier B.V. All rights reserved.

Keywords: Aluminium nitride; Diamond; Sputtering

1. Introduction

The increasing volume of information and communication media, such as mobile telephones and satellite services, has brought to a growing demand of high-performance surface- and bulk-acoustic-waves devices, operating in the gigahertz range of frequencies. For such applications use of piezoelectric films of aluminium nitride is very attractive because of its high acoustic wave velocity, substantial electromechanical coupling coefficient and good temperature stability, together with excellent mechanical and chemical properties [1–3].

On limiting our attention to surface-acoustic-wave (SAW) devices, AlN films have been successfully utilized on substrates showing high SAW phase velocity, such as silicon and sapphire to implement filters and resonators operating at high-frequency [4–9]. From this point of view, thick diamond films as substrates for SAW devices are very attractive because of their high sound velocity, the highest observed among all materials, which allows higher frequency operation at a given interdigital transducer line-width resolution technology. On the other hand, AlN is an ideal piezoelectric layer for diamond-based SAW applications, as its high acoustic wave velocity, the highest among all piezoelectric materials, better matches that of diamond. Moreover the AlN/diamond structure exhibits smaller velocity dispersion with respect to other piezoelectric films [10–16].

AlN films have been grown on a variety of substrates using different deposition methods including chemical vapor deposition techniques [17,18], molecular beam epitaxy [19], laser ablation and reactive sputtering techniques [20–25]. Among these methods, sputtering techniques allow to obtain *c*-axis oriented AlN films with small surface roughness at relative low temperatures [26]. The correlation between the conditions of the sputtering process and the structure characteristics of the films obtained has been widely investigated, even though the results published are sometimes conflicting. This is probably due to the complexity of the sputtering process, to an inadequate validation of the models and to a lack in the comparison between models. Specifically for applications to

* Corresponding author.
E-mail address: enrico.verona@idac.rm.cnr.it (E. Verona).

0040-6090/$ - see front matter © 2005 Elsevier B.V. All rights reserved.
doi:10.1016/j.tsf.2005.10.073

SAW devices, the orientation of the c-axis of the AlN film must be perpendicular to the substrate surface. Consequently, the comprehension of the origin of preferred orientation is of crucial importance. The preferred orientation is caused by anisotropy of certain properties, such as surface energy or reactivity, depending on the crystallographic plane of the deposited materials and influence the film formation processes. Therefore many studies tried to relate such anisotropies to film formation processes that finally determine the preferred orientation [27].

The main process parameters that affect the growth of AlN films are: the thickness of the film, the bias voltage, the sputtering power, the gas mixture, the gas pressure, the target-substrate distance and the temperature of the substrate.

In this work we focus our attention on the growth of AlN thin films on diamond substrates by radio frequency (RF) reactive diode sputtering technique. Energy dispersive X-ray diffraction (EDXD) and reflectivity techniques [28–32] were used to investigate the growth behavior at various substrate temperatures leaving all the other process conditions unchanged. Highly textured films were obtained with c-axis perpendicular to the diamond substrate showing good reproducibility and extremely smooth surfaces, which is an extremely important feature for low loss SAW propagation.

2. Experimental section

2.1. AlN films deposition

The AlN films were deposited by RF reactive diode sputtering technique, using a commercial MRC 8620 sputtering head and a cryogenic vacuum system. The sputtering conditions were as follows: RF power 500 W, target 6″ Al (purity 99.999%), substrate to target distance 5 cm, gas composition 99.999% pure N_2 at a pressure of $3 \cdot 10^{-3}$ Torr controlled, at a constant flow rate of 90 sccm, by an MKS 647A gas flow controller (Fig. 1). Several sputtering runs were carried out at various temperature with substrates heated in the range 200 to 500 °C, in order to evaluate the most favourable deposition conditions. The background pressure of the system was better then $1 \cdot 10^{-7}$ Torr; a 30-min pre-sputtering in 100% N_2 was performed before each deposition run, followed by 1 to 2 h of thermal annealing and slow cooling. The main deposition conditions followed during the sputtering runs are reported in Table 1.

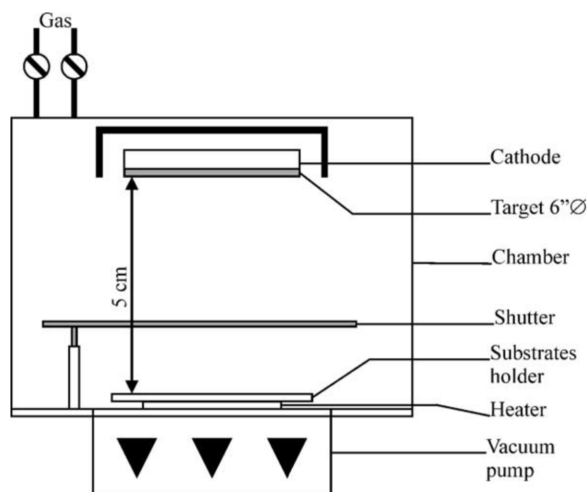

Fig. 1. Schematic drawing of the sputtering system.

Table 1
AlN sputtering conditions

RF power	500 W
Substrate temperature range	200 to 500 °C
Gas pressure	$3 \cdot 10^{-3}$ Torr
Gas composition	100% 99.999 pure N_2
Gas flow rate	90 sccm
Target	Al 99.999 pure 6″ diameter
Target substrate distance	~50 mm
Growth rate	0.3 μm/h
Background pressure	$<1 \cdot 10^{-7}$ Torr

The diamond/Si substrates, provided by Sumitomo Chemicals Japan, consisted of 2″ polycrystal Si wafers, ~800 μm thick, coated with a 23 μm thick diamond layer with the free surface optically polished. The substrates used to perform the AlN deposition tests where 5 × 5 mm squares, sliced from the wafers. Before being introduced into the sputtering chamber, all the samples were carefully cleaned using a standard cleaning procedure including detergent bath soak, DI water rinse and drying, followed by exposure to an O_2 (purity 99.999%) plasma in order to remove residual organic contaminants, for 3 min, at an RF power of 200 W and a pressure of 100 mTorr.

2.2. Diffractometer/reflectometer

A schematic sketch of the energy dispersive non-commercial diffractometer/reflectometer used in the present work is shown in Fig. 2 [33]. The non-monochromatized (*white*) primary beam is produced by a W anode X-ray tube and is collimated by two tungsten slits upon the sample which is placed in the optical centre of the instrument. Two more slits define the acceptance angle of the detector selecting a small portion of the diffracted beam. The detector is an EG and G ultra pure Ge solid-state device, capable to perform the energy scan of the diffracted photons. In this way the reciprocal space scan, necessary to collect the diffraction pattern, is carried out electronically rather than mechanically as in the ordinary *angular-dispersive* X-ray diffraction. The energy resolution is about 1.5% with a maximum count rate of 10 kcounts/s. Source and detector arms are moved by two linear actuators driven by step motors, leading to a minimum scattering angle increment and reproducibility of 0.002°.

2.3. Experimental methods

The experimental set-up described above was used to measure the rocking curves of all the samples, allowing the investigation of their structural properties. In an X-ray

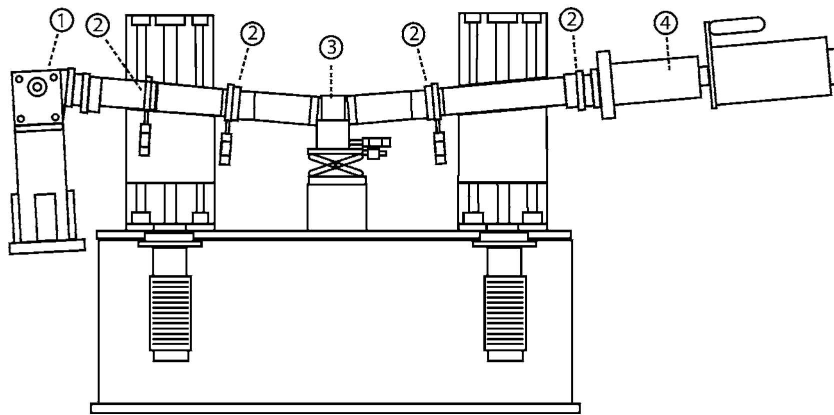

Fig. 2. Schematic drawing of the energy dispersive X-ray diffractometer: (1) X-ray W anode tube; (2) collimation slits; (3) sample position; (4) Ge single crystal solid state energy sensitive detector.

diffraction experiment the intensity of the radiation collected at the detector is a function of the scattering parameter $q = aE\sin\vartheta$ where 2ϑ is the deflection angle, E the energy of the X-ray beam used for the measurement and $a = 1.014$ Å^{-1}/keV [34]. This means that two different possibilities to perform a q scan are possible: to make an angular scan, keeping the energy fixed (*Angular Dispersive Mode* — AD) or to keep the experimental set-up fixed and make use of the *bremmsstrahlung* white beam (*Energy Dispersive Mode* — ED). In this way, the diffraction angle is fixed before starting the measurements. After this, the machine geometry is no longer modified and the data collection is performed in stationary conditions.

In the ED diffraction mode, the whole diffraction pattern is obtained in a single measurement, providing a fast recording of films Bragg peaks and, consequently, of their rocking curves. This is particularly useful when thin films are to be investigated or, in general, samples of small size. Moreover the fixed geometry, not requiring any mechanical movement, makes the measurements extremely accurate and reproducible, not being affected by possible systematic errors induced by the angular scan. A full description of the EDXD method, together with a detailed discussion of its advantages, is reported elsewhere [34].

3. Experimental results

AlN films are polycrystalline with a wurtzite hexagonal structure, showing a preferred orientation of the c-axis along the normal to the substrate surface. The aim of this work was to find out the best conditions to grow the films along this direction, corresponding to the <002> AlN reflection, minimizing the contributions of the domains oriented in different directions.

The first step consisted of collecting a diffraction pattern of the diamond/Si substrate, to confirm the polycrystalline nature of the silicon component, the presence of the diamond deposited on it and the accuracy of our measurements compared to literature data. Fig. 3 reports the q range of the pattern, showing the presence of silicon domains oriented along different directions: (1) Si <111> at $q = 2.039$ Å^{-1}, (3) Si <220> at $q = 3.277$ Å^{-1}, (4) Si <311> at $q = 3.838$ Å^{-1}; all these values are in good agreement with published data [35]. In the inset, the q range containing the diamond signal is expanded, to point out the presence of the diamond <111> reflection at $q = 3.056$ Å^{-1}, and to show the intensity ratio between the two materials that form the substrate.

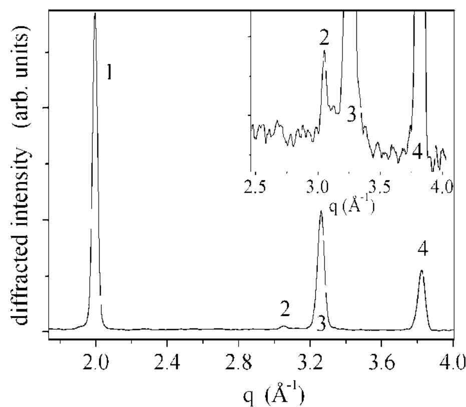

Fig. 3. Diffraction pattern of the diamond/Si substrate. These reflections of the polycrystalline Si are visible: (1) Si <111>; (3) Si <220>; (4) Si <311>. In the inset the diamond DLC <111> reflection (2) is highlighted.

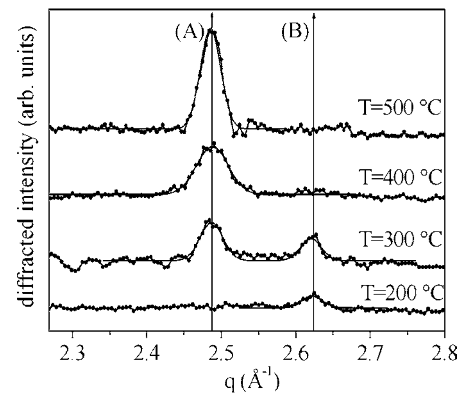

Fig. 4. Diffraction patterns of AlN films grown at different temperatures as a function of the scattering parameter: (A) AlN <002>, (B) AlN <101>. Increasing the temperature, the desired <002> reflection gets dominant and the <101> signal progressively tends to disappears.

In Fig. 4, the diffraction patterns of a set of AlN thin films deposited on diamond/Si substrates in different heating conditions of the substrate are shown. The peck at $q = 2.485$ Å^{-1}, indicated as (A), corresponds to the AlN <002> reflection, while the one at $q = 2.625$ Å^{-1}, (B), can be assigned to the AlN <101> reflection, as expected.

Passing from the sample deposited at 200 °C up to the one deposited at 500 °C, a progressive enhancing of the AlN <002> reflection can be noticed as well as the disappearance of the <101> AlN reflection, considered undesirable in order to obtain a good surface wave transducer. In fact, at 200 °C no evidence of any preferred orientation along the c-axis is observable; at 300 °C the AlN is still polycrystalline and the contributions of the two domains are comparable; at 400 °C and, more evidently, at 500 °C the film shows to be oriented along the <002> privileged direction. Moreover, the <002> Bragg peak gets higher and narrower as the deposition temperature is increased.

Then, to find out the statistical distribution of the orientation of these <002> domains, i.e. the degree of epitaxy of the c-axis oriented AlN film, a rocking curve analysis was performed. The measurements were carried out by recording the intensity of the diffracted radiation as a function of the asymmetry parameter $\alpha = (\theta_i - \theta_r)/2$ while the scattering angle 2θ was kept unchanged. Each point of a rocking curve, i.e. the value in correspondence of a generic α, is calculated as the ratio between the intensity of the Bragg peak in correspondence of that α-value with respect to the maximum intensity of the same peak along the α-scan. In this way no normalization to the primary X-ray beam spectrum, usually required in EDXD measurements, is necessary. The peaks on the diffraction pattern are fitted by the sum of a Gaussian and a linear function to model, respectively, the convolution of the Bragg peak with the diffractometer transport function and the almost flat background (containing also the Compton contribution) [36]. The integral of the Gaussian components are used to calculate the rocking curve. In the case of the ED mode, since the diffraction pattern is collected in parallel at any q value, all the rocking curves of the peaks visible in the explored q range are collected simultaneously [35–38]. This means that all the

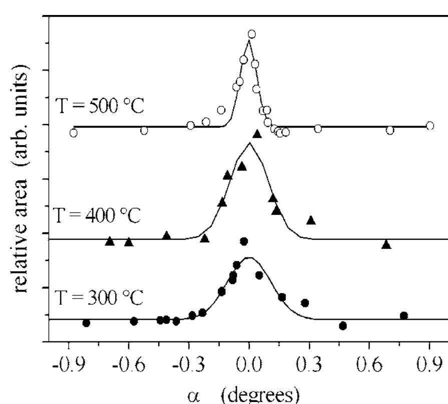

Fig. 5. Rocking curve analysis of the AlN <002> reflection is reported as a function of the sample growth temperature. The red line is a Gaussian fit of the rocking curves: the FWHM is reduced as the temperature increases.

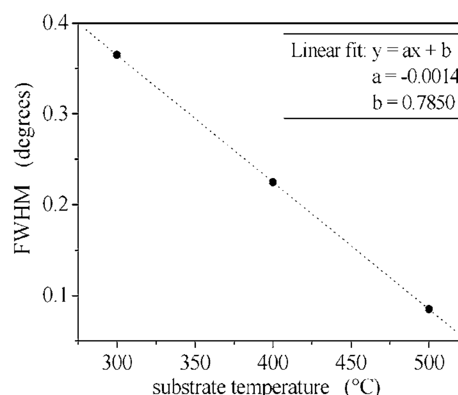

Fig. 6. The trend of the FWHM of the rocking curves, deduced from the Gaussian fit, is plotted as a function of the deposition temperature (dots) and fitted by a linear function (straight line).

structural information about Si, diamond, and AlN were collected in a single set of measurements. The two substrate components exhibit a flat-top rocking curve, since the domains are all randomly oriented.

In Fig. 5, the rocking curves relative to the AlN <002> reflection are shown for the samples grown at a deposition temperature of 300, 400 and 500 °C. The rocking curves are fitted by a Gaussian curve, as well; the epitaxy degrees are deduced by the mean values of fit full width at half maximum (FWHM) of the rocking curves of all the Bragg reflections associated to each family of lattice planes (Fig. 6).

For all of them, when the asymmetry value α increases, the peak intensity decreases quite rapidly, showing a good crystalline quality of the films. In particular, the higher the temperature is, the better the AlN growth is, as can be observed in Fig. 6. The relationship between the substrate temperature, at which the AlN films are grown, and their degree of epitaxy can be described by the linear function: $y = 0.750\ (5) - 0.014\ (5)x$. Moreover, the X-ray reflectometry analysis revealed that the films are characterized by very low surfaces roughness, below 20 Å, as required for SAW applications.

4. Conclusions

Highly textured and well reproducible AlN films were grown with c-axis perpendicular to the diamond substrate. They show an extremely smooth surface, feature very important for Rayleigh waves propagation. The systematic EDXD structural characterization revealed that both the films mosaicity and their degree of epitaxy are enhanced by increasing the substrate deposition temperature. In particular, when the deposition is performed above the threshold temperature of 300 °C, AlN films with a preferential <002> orientation and characterized by a very narrow rocking curve (i.e. highly oriented) are obtained.

Acknowledgements

The work has been supported by the FISR project of the Italian Minister for Education, University and Research (MIUR).

References

[1] H.L. Kao, P.J. Shih, Chun-Hsi Lai, Jpn. J. Appl. Phys. 38 (1999) 1526.
[2] C.H. Wu, W.Y. Chiu, H.L. Kao, Electron. Lett. 37 (4) (2001) 253.
[3] M.B. Assouar, O. Elmazria, L. Le Brizoual, M. Belmahi, P. Alnot, Proceedings of the IEEE International Frequency Control Symposium and PDA Exhibition, 2002, p. 334.
[4] K. Tsubouchi, K. Sugai, N. Mikoshiba, Proceedings of the IEEE Ultrasonics Symposium, Chicago, U.S.A., October 14–16, 1981, p. 375.
[5] J.K. Liu, K.M. Lakin, K.L. Wang, J. Appl. Physi. 46 (1975) 3703.
[6] Kazuo Sato, Shun-Ichi Umino, Kazuo Tsubouchi, Nobuo Mikoshiba, Proceedings of the IEEE Ultrasonics Symposium, San Francisco, U.S.A., October 16–18, 1985, p. 192.
[7] A.J. Shuskus, T.M. Reeder, E.L. Paradis, Appl. Phys. Lett. 24 (1974) 155.
[8] C. Caliendo, G. Saggio, P. Verardi, E. Verona, Proceedings of the IEEE Ultrasonics Symposium, Baltimore, U.S.A., October 31–November 3, 1993, p. 249.
[9] H.M. Liaw, F.S. Hickernell, Proceedings of the IEEE Ultrasonics Symposium, Cannes, France, November 1–4, 1994, p. 375.
[10] H. Nakahata, K. Higaki, S. Fujii, A. Hachigo, H. Kitabayashi, K. Tanabe, Y. Seki, S. Sikata, Proceedings of the IEEE Ultrasonics Symposium, Seattle, U.S.A. November 7–10, 1995, p. 361.
[11] E.L. Adler, L. Solie, Proceedings of the IEEE Ultrasonics Symposium, Seattle, U.S.A. November 7–10, 1995, p. 341.
[12] K. Yamanoukhi, S. Sakurai, T. Satoh, Proceedings of the IEEE Ultrasonics Symposium, Montreal, Canada, October 3–6, 1989, p. 351.
[13] H. Nakahata, A. Hachigo, K. Itakura, S. Sikata, Proceedings of the IEEE Ultrasonics Symposium, San Juan, Puerto Rico, October 22–25, 2000, p. 349.
[14] A. Hachigo, H. Nakahata, K. Itakura, S. Fujii, S. Sikata, Proceedings of the IEEE Ultrasonics Symposium, Caesars Tahoe, U.S.A., October 17–20, 1999, p. 325.
[15] A. Hacigo, D.C. Malocha, S.M. Richie, Proceedings of the IEEE Ultrasonics Symposium, Seattle, U.S.A., November 7–10, 1995, p. 371.
[16] O. Elmazria, V. Mortet, M. El Hakiki, M.B. Assouar, M. Nesladek, P. Alnot, Proceedings of the IEEE Ultrasonics Symposium, Munich ,Germany, October 8–11, 2002, p. 136.
[17] M. Kishi, M. Suzuki, K. Ogawa, Jpn. J. Appl. Phys. 31 (1992) 1153.
[18] J.H. Edgar, Z.J. Yu, B.S. Sywe, Thin Solid Films 204 (1991) 115.
[19] S. Karmann, H.P.D. Schenk, U. Kaiser, A. Fissel, Wo Richter, Mater. Sci. Eng., B, Solid-State Mater. Adv. Technol. 50 (1997) 228.
[20] P. Bhattacharya, D.N. Bose, Jpn. J. Appl. Phys. 30 (1991) 1750.
[21] V. Mortet, M. Nesladek, J. D'Haen, G. Vanhoyland, O. Elmazria, M.B. Assouar, P. Alnot, M. D'Olieslaeger, Phys. Status Solidi, A Appl. Res. 193 (2002) 482.
[22] M. Ishihara, T. Nakamura, F. Kokai, Y. Koga, Diamond Relat. Mater. 11 (2002) 408.
[23] Kuo-Sheng Kao, Chien-Chuan Cheng, Ying-Chung Chen, IEEE Trans. Ultrason., Ferroelectr. Freq. Control 49 (2002) 345.
[24] Kuo-Sheng Kao, Chien-Chuan Cheng, Ying-Chung Chen, Proceedings of the IEEE International Symposium, Honolulu, U.S.A., July 21–August 2, 2003, p. 439.
[25] C.H. Wu, W.Y. Chiu, H.L. Kao, Electron. Lett. 37 (2001) 253.
[26] H. Ming Liaw, F.S. Hickernell, IEEE Trans. Ultrason., Ferroelectr. Freq. Control 42 (1995) 404.
[27] Yuya Kajikawa, Suguru Noda, Hiroshi Komiyama, J. Vac. Sci. Technol., A, Vac. Surf. Films 21 (2003).
[28] B.C. Giessen, G.E. Gordon, Science 159 (1968) 973.
[29] K. Nishikawa, T. Iijima, Bull. Chem. Soc. Jpn. 57 (1984) 1750.
[30] S.J. Roser, R. Felici, A. Eaglesham, Langmuir 10 (1994) 3853.
[31] E. Matsubara, S. Sato, M. Imafuku, T. Nakamura, H. Koshiba, A. Inoue, Y. Waseda, Mater. Trans., JIM 41 (2000) 1379.
[32] C. Park, M. Saito, Y. Waseda, N. Nishiyama, A. Inoue, Mater. Trans., JIM 40 (1999) 491.
[33] R. Caminiti, C. Sadun, V. Rossi Alberini, F. Cilloco, Patent No. 01261484, Italy, 1993.
[34] R. Caminiti, V. Rossi Albertini, Int. Rev. Phys. Chem. 18 (1999) 263.
[35] V. Rossi Albertini, B. Paci, S. Meloni, R. Caminiti, L. Bencivenni, J. Appl. Crystallogr. 36 (2003) 43.
[36] G.A. Jeffrey, G.S. Parry, R.L. Mozzi, J. Chem. Phys. 25 (1956) 1024.
[37] B. Paci, A. Generosi, V. Rossi Albertini, E. Agostinelli, G. Varvaro, D. Fiorani, Chem. Mater. 16 (2004) 292.
[38] B. Paci, A. Generosi, V. Rossi Albertini, E. Agostinelli, G. Varvaro, JMMM 272 (2004) E873.